Since January 2020 Elsevier has created a COVID-19 resource centre with free information in English and Mandarin on the novel coronavirus COVID-19. The COVID-19 resource centre is hosted on Elsevier Connect, the company's public news and information website.

Building and Environment 238 (2023) 110343

Contents lists available at ScienceDirect

Building and Environment

journal homepage: www.elsevier.com/locate/buildenv

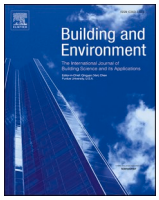

Transmission and infection risk of COVID-19 when people coughing in an elevator

Sumei Liu [a,*], Zhipeng Deng [b]

[a] Tianjin Key Laboratory of Indoor Air Environmental Quality Control, School of Environmental Science and Engineering, Tianjin University, Tianjin, 300072, China
[b] Department of Mechanical & Aerospace Engineering, Syracuse University, Syracuse, NY, 13244, United States

ARTICLE INFO

Keywords:
Disease transmission
SARS-COV-2
Enclosed space
CFD
Infection risk

ABSTRACT

People in cities use elevators daily. With the COVID-19 pandemic, there are more worries about elevator safety, since elevators are often small and crowded. This study used a proven CFD model to see how the virus could spread in elevators. We simulated five people taking in an elevator for 2 min and analyzed the effect of different factors on the amount of virus that could be inhaled, such as the infected person's location, the standing positions of the persons, and the air flow rate. We found that the position of the infected person and the direction they stood greatly impacted virus transmission in the elevator. The use of mechanical ventilation with a flow rate of 30 ACH (air changes per hour) was effective in reducing the risk of infection. In situations where the air flow rate was 3 ACH, we found that the highest number of inhaled virus copies could range from 237 to 1186. However, with a flow rate of 30 ACH, the highest number was reduced to 153 to 509. The study also showed that wearing surgical masks decreased the highest number of inhaled virus copies to 74 to 155.

1. Introduction

The COVID-19 pandemic has caused widespread illness and death, as well as economic turmoil globally. As of November 1st, 2022, the World Health Organization has reported 62 million confirmed cases and 6.6 million deaths globally. Research has shown that the virus primarily spreads in enclosed, poorly ventilated, and crowded indoor spaces where people are in close proximity to each other [1–3]. Elevators are small and often have high occupancy, making it difficult to maintain social distance which could facilitate the spread of COVID-19. There have been several reported outbreaks of COVID-19 in enclosed and crowded spaces [4,5], such as in elevators [6]. As modern people taking elevators almost every day, there is growing concern about the safety of elevator rides. However, there is a lack of studies that quantify the infection risk during elevator rides. Therefore, it is important to understand the transmission and infection of SARS-COV-2 in elevators.

An infected individual can spread thousands of virus-carrying saliva particles into the air through breathing, coughing, or sneezing. These particles were expelled from the respiratory system [7,8]. The virus-laden saliva aerosols may suspend in the air for a significant amount of time [9] or travel long distances [10] depending on the airflow pattern in the surrounding spaces. Therefore, it highlights the importance of understanding how these droplets spread in enclosed spaces like elevators. In an elevator, the airflow physics generated by ventilation systems significantly impacted the airborne droplet transmission and infection [11,12]. It is essential to use mechanical ventilation to keep the air fresh and dilute any viral droplets. Unfortunately, many elevators lack this important ventilation system. According to ISO 8100–1 [13] and EN 81 [14], ventilation apertures should be installed in the elevator, with a required effective area of 2% of the floor area. However, there are no established requirements for fan settings or adequate airflow rate values. This means that elevators may not have proper ventilation systems in place to prevent the spread of airborne droplets. According to the American standard for elevators ASME A17.1 [15], fans with proper ventilation should be installed in elevators with solid enclosures and doors. However, there are no specific guidelines for the airflow rate. Therefore, adhering to elevator standards alone may not prevent the spread of COVID-19 in elevators. Apart from the ventilation system, other factors could also impact the droplet transmission, such as location of the infected person [16,17], how persons are positioned in the elevator [18], and whether the persons are wearing masks [19,20]. Therefore, it is essential to assess the likelihood of infection of COVID-19 in elevators under different ventilation rates, source locations, and person standing arrangements.

* Corresponding author.
E-mail address: smliu@tju.edu.cn (S. Liu).

https://doi.org/10.1016/j.buildenv.2023.110343
Received 31 January 2023; Received in revised form 2 April 2023; Accepted 20 April 2023
Available online 23 April 2023

A search of the literature revealed that there is a lack of studies evaluating the risk of infection and spread of SARS-COV-2 in elevators taking into account different above-mentioned factors. Shao et al. [21] have attempted to evaluate the risk of inhaling virus-containing particles of COVID-19 in elevators. They found that the infection risk was extremely low for breathing scenario but the infection risk increased proportionally for speaking scenario. However, they only simulated breathing and speaking to produce particles and only assessed the risk based on the number of particles at a specific location. Dbauk and Drikakis [22] and Biswas et al. [23] compared the influence of different ventilation conditions on droplet dispersion in the elevator. They found that the position and operation of inlets and outlets significantly influenced the airflow pattern and particle dispersion in the elevator. However, they only considered one person in the elevator cab without any other persons. Sen [24] explored the transmission of droplets in the elevator under various conditions, including different ventilation settings, different numbers of people coughing, and different directions of cough droplets. The findings showed that appropriate ventilation is necessary in elevators. However, this investigation only used extremely simple rectangular boxes to present the three persons without considering different standing postures. In our previous research [25], we used dynamic mesh in CFD simulation to investigate how a person's movements affected particle transmission when entering or exiting a car cabin. We evaluated the exposure of other persons to particles throughout the entire elevator ride, but our focus was limited to particles exhaled from the normal breathing of the infected person. Du et al. [26] explored the virus transmission and risk of infection in elevators. They found that the risk was generally low because of the short duration of the elevator ride. But they only considered one specific standing scenario and fixed the source position. While in reality, the infected person may appear in different locations within the elevator and have varying relative positions to other persons. The effectiveness of face masks in reducing the spread of respiratory viruses was supported by several epidemiological studies [27,28]. In addition, various investigations [26,29] have explored the effect of wearing masks on reducing the infection risk. Deng and Chen [29] measured and simulated the mass of droplets inhaled by a susceptible manikin wearing a mask with different social distances. They found that the distance can be reduced to 0.5 m when people wear masks. Du et al. [26] found that when the infected person coughed, mouth covering thoroughly could reduce the virus intake of others by 85%–93%. However, limited investigation examined the effect of wearing masks on the transmission of COVID-19 in elevators.

Previous studies have not thoroughly examined the impact of ventilation rates, the position of the infected person, the location of persons, and wearing masks on the transmission and risk of COVID-19 in elevators. Their scope was limited. This paper aims to (1) investigate how easily the virus spreads through coughing droplets in elevators and assess the risk of infection for others, and (2) examine how source location, posture, and airflow rate impact the amount of virus inhaled by susceptible persons. Our previous investigation [25] found that the inhaled particle by susceptible persons was insignificant when considering normal breathing alone. Therefore, this investigation focused on the transmission of SARS-COV-2 through coughing.

The structure of this paper is as follows: In section 2, we will provide a detailed description of our research method, including information on the case design, boundary conditions, and numerical procedure. In section 3, we will present the results from our CFD model verification and analysis of various cases. In section 4, we will discuss the limitations and potential future works. Finally, we draw the conclusions in Section 5.

2. Research method

This section outlines the design of our case study, the parameters taken into account, and how we calculated the amount of virus inhaled by susceptible persons in an elevator. We will also explain the simulation techniques used to assess the transmission and infection risk when an infected individual is present in the elevator.

2.1. Case design

To investigate the transmission of SARS-COV-2 in an elevator, our simulation assumed a 120-s elevator ride in a cab with a capacity of 1600 kg (or up to 12 people) and a typical size of 2.0 m × 1.65 m x 2.5 m, which was similar to typical elevators in commercial and residential buildings. Fig. 1 shows the geometry model of the elevator cab and persons. The air flow into the cab was through inlets on the ceiling and out of the cab through outlets near the floor. The widths of the inlet and outlet were 0.05 m and 0.011 m, respectively, which were based on previous investigations [25,26]. The COVID-19 pandemic has made more people conscious of the importance of social distancing. Therefore, people tend to wait for the next elevator if the current one is already full. In addition, the number of people in an elevator is typically limited outside of rush hours. Therefore, we assumed that five people were standing still inside the cab. They were all 1.7 m tall with a total skin surface area of 2.1 m^2. From our on-site observations of people taking an elevator, we noticed that people generally stand facing the elevator door upon entering. Some people prefer to stand with their backs against the elevator wall. Due to the limited space, people usually do not stand facing each other. Therefore, we assumed two common standing postures in this investigation, as shown in Fig. 1(a) and (b). Standing scenario I represents all people facing the elevator door. Standing scenario II represents everyone standing against the walls. Because the geometry of the elevator cabin was nearly symmetrical, the infected person was assumed to locate at positions A, C, and D, as shown in Fig. 1(c). These three source locations represent the front, middle, and back positions of the elevator source. The simulation also considered two ventilation rates, 3 ACH and 30 ACH [30], to represent infiltration and mechanical ventilation, respectively. ACH means how many cubic feet of air can be provided every hour divided by the volume of the room. The volume of the elevator was 8.3 m^3.

The case design used in this study was summarized in Table 1. Case 1 was the baseline case, which was a common scenario with low ventilation. The ventilation rate in Case 1 was as low as 0.007 m^3/s by only infiltration. Person A was infected in standing scenario I. The first set of cases 1 to 5 were designed to investigate various standing positions and source locations. Note that in the standing posture I, when person D was the infected person, most particles would be deposited on the elevator wall in front of person D due to the short distance. This would result in a low infection risk via airborne droplets. Therefore, we only simulated case 5 under standing posture II with person D infected. In the second set of cases 6 to 10, we used an airflow rate of 0.069 m^3/s by mechanical ventilation, which corresponded to 12 CFM (cubic feet per minute) for each person when the capacity was 12. The second set of cases repeated the same source locations and standing positions as the first set. We also investigated the effect of wearing masks on the amount of virus inhaled by persons in the elevator. In cases 11 to 13, the positions and postures of the other persons were kept the same as in cases 2, 4, and 5, but the infected person was assumed to be wearing a surgical mask. This investigation only simulated three cases to explore the impact of wearing masks on inhaled virus load. This is because the inhaled virus copies can be scaled by using the reduction efficiency for other scenarios.

2.2. Boundary conditions

In order to accurately evaluate the risk of SARS-COV-2 transmission in an elevator, it is important to provide accurate source information about how the virus was propelled into the air. A COVID-19 patient could expel the SARS-COV-2 virus through the exhalation of respiratory droplets. This study focused on how the virus was spread through coughing in the elevator, as our previous investigation [25] found that

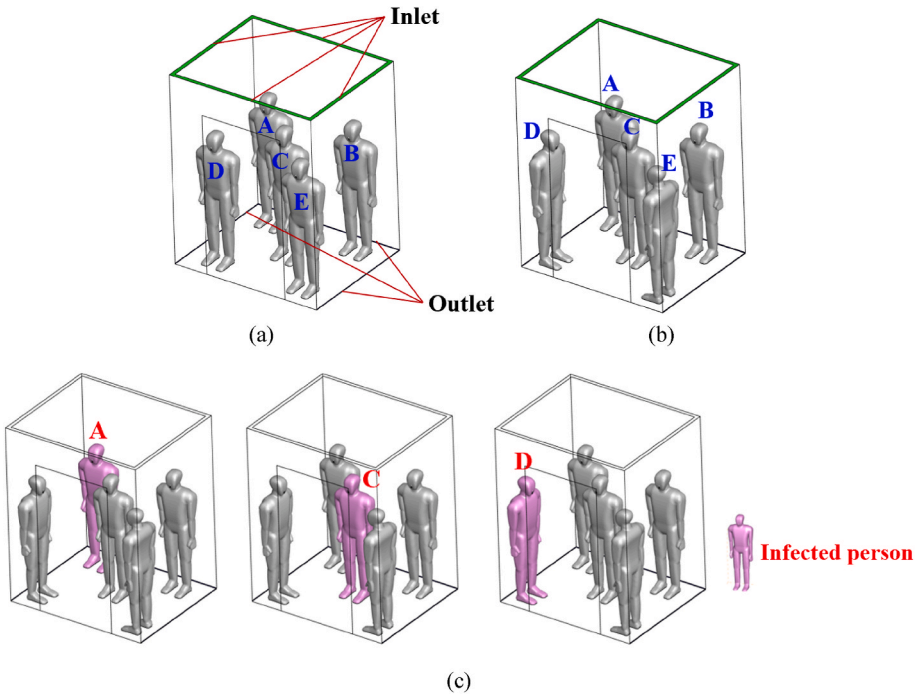

Fig. 1. Geometry model of the elevator and persons: (a) standing posture of scenario I – all persons facing the elevator door, (b) standing posture of scenario II – all persons standing against the walls, (c) different source locations and infected person.

Table 1
An overview of the case design used in this study.

Case	Ventilation rate (ACH)	Flow rate (m^3/s)	Infected person location	Standing posture scenario	Protection
1	3	0.007	A	I	None
2	3	0.007	A	II	None
3	3	0.007	C	I	None
4	3	0.007	C	II	None
5	3	0.007	D	II	None
6	30	0.069	A	I	None
7	30	0.069	A	II	None
8	30	0.069	C	I	None
9	30	0.069	C	II	None
10	30	0.069	D	II	None
11	3	0.007	A	II	Surgical Mask
12	3	0.007	C	II	Surgical Mask
13	3	0.007	D	II	Surgical Mask

breathing alone did not contribute significantly to the spread of the virus. To introduce the particles into the airflow field, we first need to obtain the size spectrum of droplets due to coughing. This investigation used the particle data from previous research by Chao et al. [31] and Yang et al. [32]. The data from Chao et al. did not include droplets smaller than 1 μm, while Yang et al. measured particles smaller than 3 μm. To account for this, this study used data from Yang et al. for particles smaller than 3 μm. The respiratory droplets are initially wet by nature. Then they would evaporate and finally become "droplet nuclei", which can remain airborne for long periods of time and spread widely following the airflow pattern [31]. Many investigations [33,34] have studied the process of droplet evaporation into droplet nuclei. Previous investigation [35] has found that droplets smaller than 30 μm did not significantly evaporate while large droplets were prone to settling and difficult to inhale. Therefore, this study did not take into account droplet evaporation. It was important to note that the particle sizes provided by Chao et al. [31] were wet droplets. This investigation further converted the wet droplet sizes into dry particles according to Nicas et al. [36]. Table 2 summarized the cough-generated particle sizes and numbers by Chao et al. [31] and Yang et al. [32]. Chao et al. [31] used interferometric Mie imaging to measure the droplet size in close proximity to the mouth to avoid air sampling losses. Eleven volunteers were asked to cough 50 times during the test. The average droplet number count per person was summarized in their investigation which can be assumed typical. This investigation assumed that the infected person only coughed once during the entire 120-s elevator ride. The coughing occurred at 0.5 s, which was at the beginning of the 120-s ride. Therefore, the particles were emitted from the infected person's mouth at 0.5s.

The virus load, the amount of virus in the droplets, was a key factor in determining the relative contribution of SARS-COV-2 transmission. This investigation used the following equation to calculate the virus load N_d in droplets of different diameter d:

Table 2
Size distribution and the number of virus copies in the droplet's nuclei by coughing.

Diameter (μ m)	Number of droplets [31,32]	Number of virus copies [38–40]
0.75	140,000	0.43
1.32	71	5
2.64	974	41
5.28	362	80
8.8	119	370
12.32	44	1
15.84	42	3
19.8	36	6
27.5	36	15
38.5	25	42
49.5	30	89
60.5	28	163
77	78	337
99	44	716
165	37	3313
330	25	26,507

$$N_d = C_d \times \frac{\pi d^3}{6} \quad (1)$$

where d refers to the diameter of the wet droplet, C_d is the corresponding viral concentration. Johnson et al. [37] found that droplets larger than 20 μm mainly originated from the mouth. While those smaller than 20 μm came mainly from the respiratory tract. Recent research [38,39] has revealed the viral concentration in saliva and sputum. Generally, the saliva comes from the mouth, and sputum from the respiratory tract. Consequently, droplets larger than 20 μm were found to have a viral concentration of 1.2×10^8 copies/mL, while those smaller than 20 μm had a viral concentration of 1.34×10^{11} copies/mL. This investigation further calibrated the viral concentration for droplets less than 20 μm based on the data from Lindsley et al. [40]. The authors found that 35% of the viral concentration was in droplets smaller than 4 μm, 23% was in particles from 1 to 4 μm, and 42% was in particles smaller than 1 μm. This investigation calibrated the viral load by keeping the same amount of total virus concentration for small particles $<20\ \mu$ m. The calculated viral copies are also consistent with previous investigations [24,41]. Table 2 summarizes the number of virus copies in the droplet's nuclei due to coughing.

Simulating how particles transmitted in an elevator required not only accurate information about the amount of virus present but also the thermal fluid characteristics from the persons. This investigation used the flow characteristics of coughing and breathing from Gupta et al. [42,43]. Fig. 2(a) and Fig. 2(b) show the air velocity profile and the jet direction by coughing. Fig. 2(b) shows the change in airflow when the persons started breathing through the nose according to [42]. In reality, all the persons would breathe differently. Therefore, this investigation used different patterns of asynchronous breathing for each person. Gupta et al. [42] conducted measurements to obtain the breathing flow rate, flow direction, and area of mouth/nose opening and developed the equations to express the breathing flow rate. This investigation used the same equations as Gupta et al. [42] to generate random amplitude and frequency of the breathing sine wave. Fig. 2(b) depicts the random patterns of breathing air velocity assigned to each person's nose. The mouth of the infected person was assigned for coughing, while the nose was assigned for breathing. For the other individuals who only breathed, their mouths were assumed to be closed, and only their nose breathing airflow was simulated. The effect of wearing masks on particle transmission was also simulated, where the mask significantly reduced the coughing velocity and filtered the cough-generated particles. Due to the complexity of the simulation model, a simplified method was used to represent the mask's blocking effect. The coughing velocity and particle droplets after passing through the mask were directly assigned as boundary conditions for the person's mouth. The velocity of coughing with a surgical mask can be described as two jets with upward and forward directions according to Chen et al. [44], as shown in Fig. 2(c). A filtration efficiency from Pan et al. [45] was applied to the cough-generated particles. The filtration efficiencies for particle sizes of 0.75 μm, 1.32 μm, 2.64 μm, and 5.28 μm were 67.3%, 73.0%, 78.0%, and 93.0%, respectively. All particles larger than 5.28 μm were filtered. When particles reached the nose of each person, the particles were inhaled by the corresponding person when the breathing status is inhaling. The accumulated virus copies inhaled by each fellow person by breathing could be sampled through the nose of each person along time. This investigation adopted the accumulated inhaled virus dose inhaled over time to assess the infection risk for the susceptible persons.

Table 3 lists the boundary conditions for Case 1. The airflow rate was 0.007 m^3/s. The air coming into the elevator had a velocity of 0.02 m/s and a temperature of 28 °C. The air flows into the elevator perpendicular to the inlet surface. The surface temperature of the persons, who were dressed, was measured at 31 °C [46]. The elevator walls were treated as adiabatic. For particle boundary conditions, the size distribution and number of particles due to coughing can be found in Table 2. The trap boundary was used for all the walls, which presumed no particle

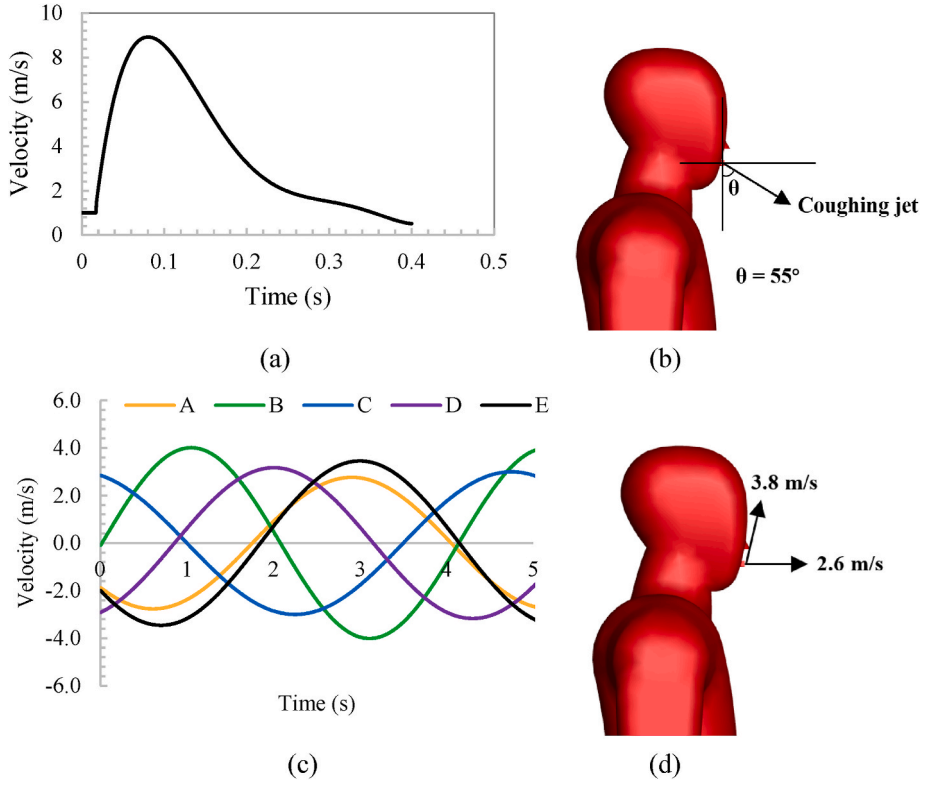

Fig. 2. The fluid boundary conditions: (a) coughing velocity produced by the infected person [43]; (b) the coughing jet direction, there was a downward angle based on Gupta et al. [43]; (c) the air velocity of asynchronous breathing distributions [42] assigned at the nose of each person. For subsequent times, it was assumed that breathing would fluctuate periodically; (d) coughing velocity with wearing a mask.

Table 3
Boundary conditions used for all considered cases.

Boundary	Type	Conditions	Particle
Human body	Non-slip wall	Temperature of 31 °C [46]	Trap
Elevator walls/ ceiling/floor	Non-slip wall	Adiabatic	Trap
Inlet	Velocity-inlet	Supply velocity of 0.02 m/s Temperature of 28 °C	Reflect
Outlet	Outflow	–	Escape
Mouth and nose of the infected person	Velocity-inlet	User-defined function in Fig. 2 Temperature of 33 °C	Reflect
Noses of the other persons	Velocity-inlet	User-defined function in Fig. 2 (b) Temperature of 33 °C	Escape

re-suspension. Therefore, particles would be deemed trapped once reach a wall surface. The particle's trajectory would end when it reached the outlet and left the computational domain, which was considered to be the escape boundary. Note that elevators usually accelerate or decelerate within a distance of one floor and reach their rated speed [47]. Since the acceleration or deceleration time is relatively short, it has been disregarded in this investigation.

2.3. Calculation of accumulated virus dose

In this study, the following equation was used to determine the number of SARS-CoV-2 droplets inhaled by susceptible persons:

$$Dose = \int_0^T \sum_d N_d \, dt$$

where N_d is the number of virus loads with a diameter of d inhaled by a susceptible person, t is time in s, and T is the length of duration in the elevator. According to Prentiss et al. [48], it took roughly 300–2000 virus copies to cause an infection. For Omicron variant, the susceptible persons would be infected if they inhaled over 400 virus copies [49].

2.4. Numerical procedure

We first ran steady state simulation for airflow distribution in the elevator where the mouths and noses of all persons were closed. Then we moved to transient simulation for coughing and breathing by using the steady state airflow as the initial airflow conditions. In this study, the RNG k-ε model [50] was used in ANSYS Fluent version 2021 to calculate the airflow and temperature fields in the elevator, which has been found to be more appropriate for indoor airflow than other RANS models [12,51]. The standard form of the governing equations is shown as:

$$\frac{\partial(\rho\overline{\Phi})}{\partial t} + \rho\overline{u_i}\frac{\partial\overline{\Phi}}{\partial x_i} - \frac{\partial}{\partial x_i}\left[\Gamma_{\varphi,eff}\frac{\partial\overline{\Phi}}{\partial x_i}\right] = S_\Phi \tag{2}$$

where Φ is the solving variables, i.e., velocity, temperature, and turbulence parameters namely turbulent kinetic energy and the dissipation rate of the turbulent kinetic energy; $\Gamma_{\varphi,eff}$ the effective diffusion coefficient, and S_Φ the source term of an equation; u_i and x_i denote the directional components for velocity and space coordinates, respectively [52,53]. The governing transport equations were discretized by means of the finite volume method. The SIMPLE algorithm was used to solve the Navier-Stokes equations. The convection and viscous terms of the governing equations were solved using a second-order discretization scheme. Furthermore, Boussinesq model was used to take into account the changes in air density. The solution was considered to have converged when the normalized residuals for all independent parameters were below 10^{-4}.

After determining the airflow pattern, this study used the Lagrangian method to calculate the trajectory of each particle by coughing based on Newton's law. This method could allow for the consideration of each particle individually and the forces between fluid and particles as

$$m_d\frac{\overrightarrow{du_d}}{dt} = \overrightarrow{F_G} + \overrightarrow{F_D} \tag{3}$$

$$\overrightarrow{F_G} = \frac{\pi d_d^3}{6}(\rho_d - \rho) \tag{4}$$

$$\overrightarrow{F_D} = \frac{C_D}{2}\frac{\pi d_d^2}{4}\rho|\overrightarrow{u_d} - \overrightarrow{u}|(\overrightarrow{u_d} - \overrightarrow{u}) \,/\, C_c \tag{5}$$

where d_p particle diameter, $\overrightarrow{u_p}$ particle velocity vector, $\overrightarrow{u}$ air velocity vector, g gravitational acceleration vector, ρ_p particle density, ρ air density, and C_c the Cunningham correction factor [54], and C_D the drag coefficient. The C_D is expressed as:

$$C_D = a_1 + \frac{a_2}{Re_d} + \frac{a_3}{Re_d^2} \tag{6}$$

where a_1, a_2, a_3 are coefficients. They are determined by the droplet Reynolds number [55]:

$$Re_d = \frac{|\overrightarrow{u_d} - \overrightarrow{u}|d_p}{\upsilon} \tag{7}$$

where υ is kinematic viscosity.

To model the turbulent dispersion of the particles, this investigation used the discrete random walk (DRW) model [56], which was one of the most widely used models for simulating particle dispersion in a turbulent flow. Note that there are 140,000 droplets with the size less than 1 μm and only 1950 droplets with the size larger than 1 μm, as Table 2 shows. The large quantitative differences would easily skew the simulation results. To accurately calculate the number of droplets and save on computational resources, two separate simulations were run: one for droplets smaller than 1 μm and one for droplets larger than 1 μm. In the simulation for smaller droplets, 140,000 particles were released into the cab from the infected person. To ensure accuracy in the simulation for larger droplets, 1950 × 100 particles were released into the cab where 1950 was the actual particle number emitted from the coughing, as shown in Table 2. This is because the DRW model used the stochastic method to simulate the turbulent dispersion of the particles. When the particle number is too small, the simulated results may not be accurate. To improve the accuracy, one solution is to repeat the simulation for several runs and further calculate the average particle concentration by using the simulated results. Another method is to increase the emitting particle number to meet the statistical criterion. Zhang et al. [57] have compared these two methods and found that by gradually increasing the particle number, the solution became more stable. Therefore, this investigation emitted 1950 × 100 particles from the coughing. The simulated virus copies were then scaled by 0.01 times to maintain the actual particle source. Finally, the results of the simulated inhaled virus copies for each person from both simulations were then added together to get the final results. The particle size distribution larger than 1 μm was set using the "DPM injections from file", where the particle diameter and particle number were listed according to Tables 2 and in Ansys Fluent.

This study used the ANSYS meshing tool to create a tetrahedral grid for the complex geometric structures of the elevator and riders in all the cases. We conducted a grid independence analysis by comparing three different grid sizes with different total grid cell numbers, including a fine mesh (5.5 million), medium mesh (2.01 million), and coarse mesh (0.99 million). Fig. 3 compares the air velocity and temperature with different meshes. The results showed that using the medium and fine meshes produced similar results. Further refinements of the meshes contributed to a negligible difference in the velocity and temperature profiles with an average relative error within 5%. So, the medium mesh was chosen for the subsequent simulations. Fig. 4 shows the grid distribution used in the elevator and the mesh near the mouth and nose of the person. The grid sizes at the mouth, nose, human body, ceiling inlet, floor outlet, and

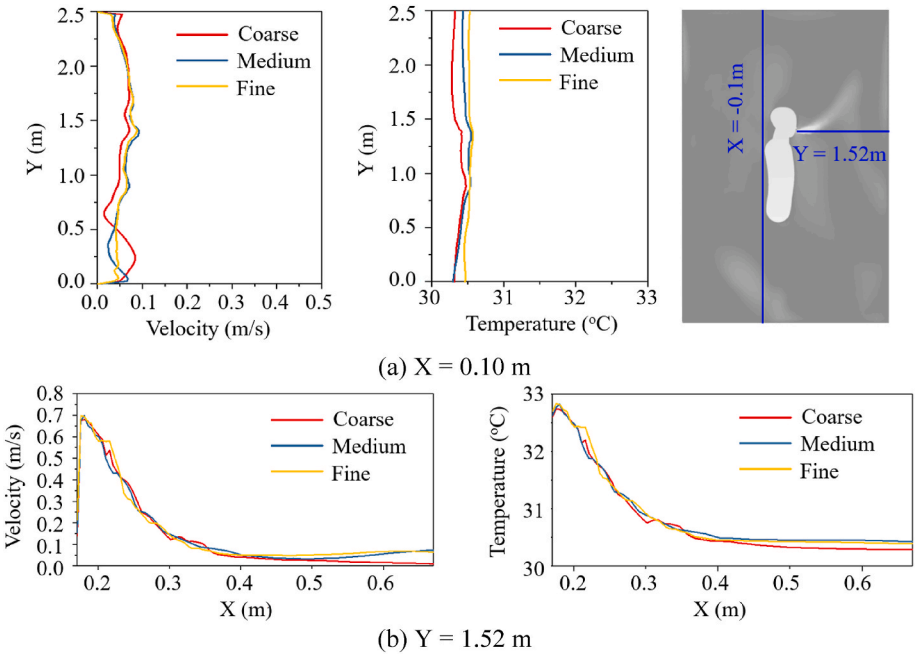

Fig. 3. Comparison of the air velocity and air temperature with different meshes at two different locations.

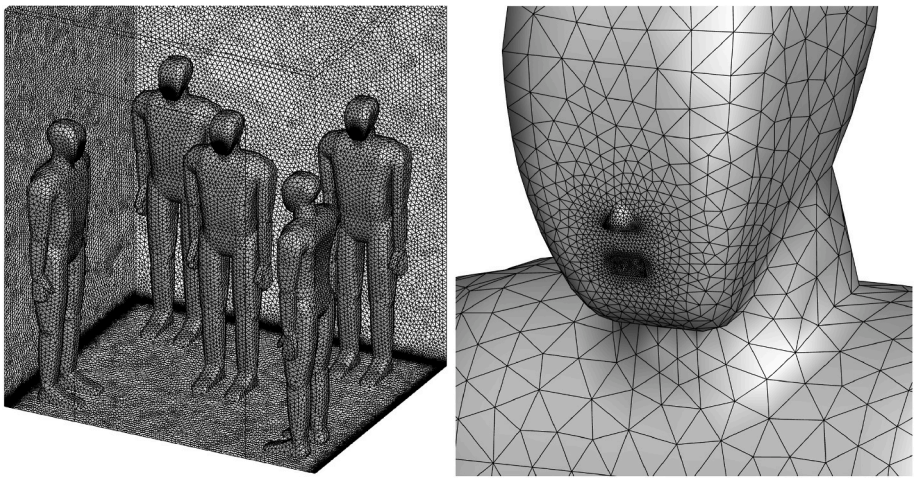

Fig. 4. Grid distribution used in this study: (a) in the elevator, and (b) near the mouth and nose of the person.

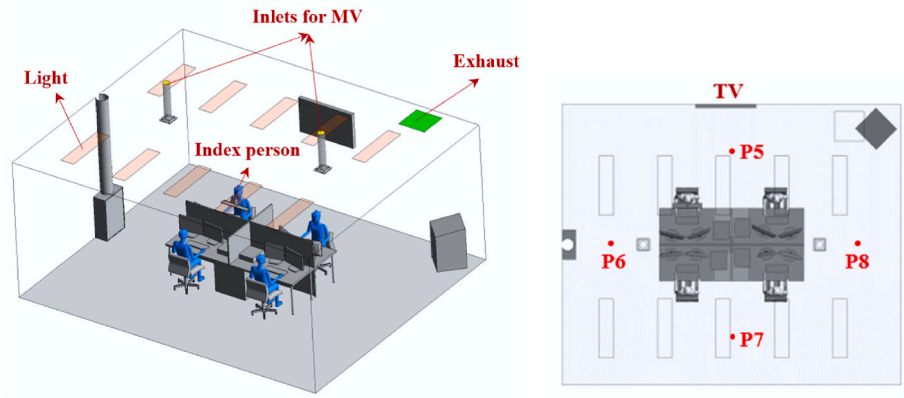

Fig. 5. The configuration of the office chamber and experimental measurement locations used by our previous investigation [58] to validate the CFD model.

elevator were 0.0015 m, 0.0015 m, 0.03 m, 0.03 m, 0.0075, and 0.03 m, respectively. A grid size function with a growth rate of 1.2 was adopted to increase the grid size gradually.

3. Results

3.1. Verification of CFD model

It is essential to assess the accuracy of the CFD model for simulating particle transmission. In this study, we first compared the results from the CFD model with data from a previous study that measured airflow and particle concentration in an office space [58]. Fig. 5 shows the geometry of the office room and the measurement locations. The office space used in the previous study had similar airflow dynamics to an elevator. Fig. 6 compares the simulated and measured temperature, velocity, and particle concentration distributions in the office. The maximum differences between the simulated results and measured data for temperature, air velocity, and normalized concentration were 1 °C, 0.01 m/s, and 1.0, respectively. This study did not consider the detail of the diffusers and some supporting structures were neglected. In addition, there were discrepancies between the simulated geometric model and the actual office structures, which could contribute to the differences observed. The results of the comparison shown in Fig. 6 indicated that the CFD model reasonably predicted the airflow and particle concentration in the office space, validating the method used in this investigation.

3.2. Simulation results of case 1

This subsection presents the results of simulating the spread of virus-laden particles caused by a single cough in an elevator (Case 1) using the verified CFD model. The results in Fig. 7 illustrate the temporal distribution of particles expelled by the infected person A (person in purple color). The figures show that large particles tend to deposit in the proximity of the infected person due to the large inertial force and airflow pattern. While smaller particles were transported by the airflow in the elevator. Additionally, Fig. 8 demonstrates that the particles tend to travel upwards due to the thermal plume formed by the people in the elevator, and that the particles eventually reach the breathing zone of person D at 20 s. The figures also show that the particles were mainly concentrated on the left side of the elevator for the first 60 s, then moved to the other side of the cab. This is because the air distribution inside the

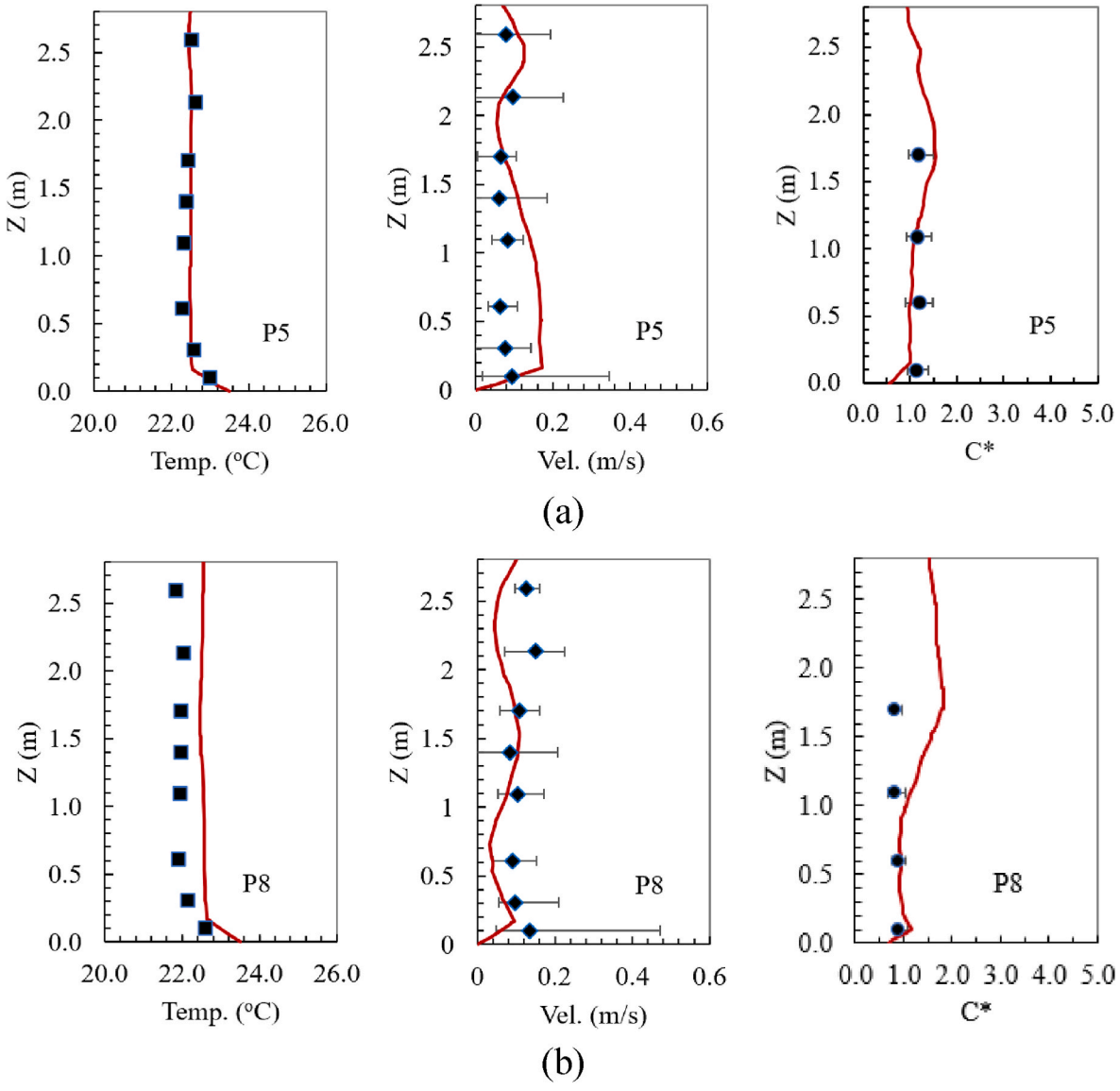

Fig. 6. Comparison of measured and calculated air temperature, velocity, and particle concentration in an office room at different measurement points. (C* the measured normalized particle concentration $(C - C_{supply})/(C_{exhaust} - C_{supply})$).

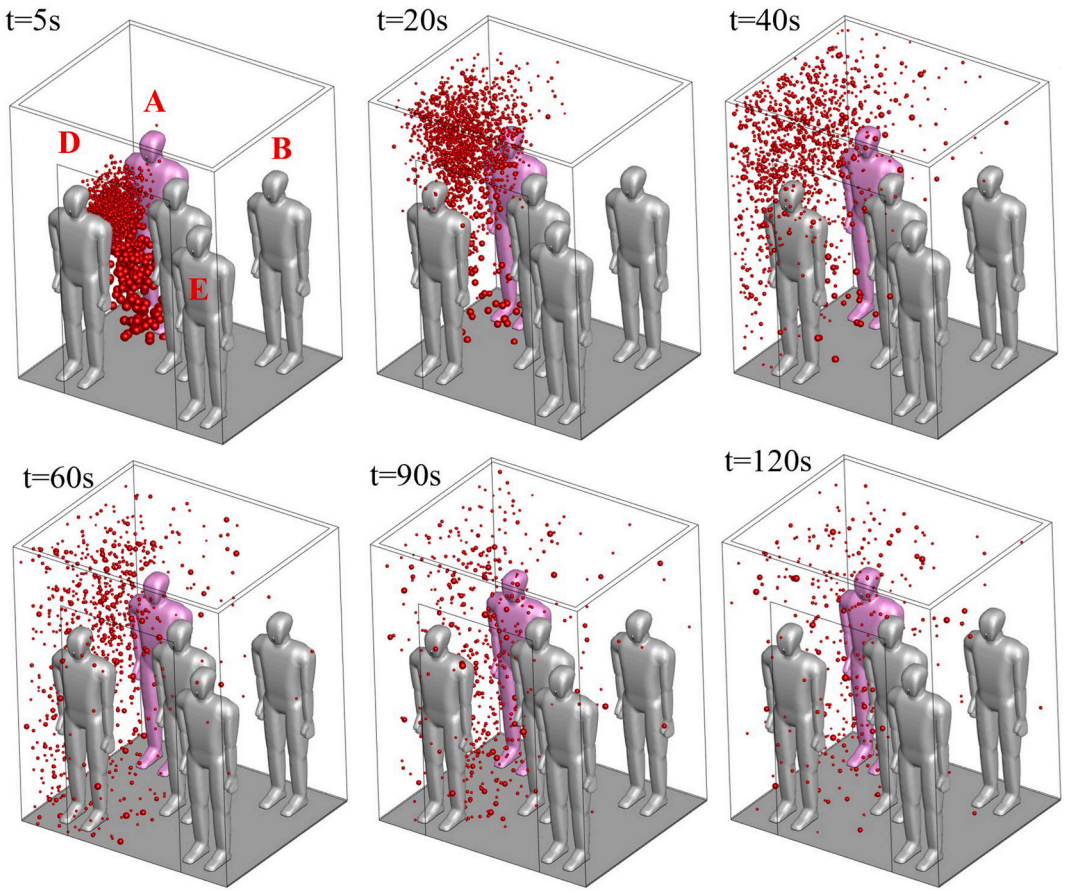

Fig. 7. Distributions of virus-laden particles expelled from a single cough in the elevator of Case 1 over time.

elevator was nearly symmetric in this case, as shown in Fig. 8. Two vortexes were formed on the upper part of the persons and some particles were still suspended in the air inside the elevator at 120 s. More detailed information on airflow distributions in the elevator of Case 1 over time can be found in Fig. A1 in Appendix I.

Fig. 9 shows the accumulated number of virus copies inhaled by each person in the baseline case. The results show that the inhaled virus dose for person D was the highest, as this person was standing in front of the infected person and the airflow brought particles into the breathing zone before being discharged through the exhausts near the floor of the elevator. The inhaled number of virus copies for person D during the 2-min elevator ride was 438, which may result in infection. While the inhaled number of virus copies for the other three persons was less than 50. Note that according to Fig. 9, there appears a nearly horizontal line between two ascending sections of the time series of the number of inhaled viruses. This is because this investigation sampled the particle number inhaled from the nose of the susceptible persons. While each breathing cycle can be divided into inhalation and exhalation. When exhaling, people are not inhaling any particles. As a result, the cumulative number of viruses inhaled will remain constant during this time.

3.3. Impact of source locations and standing positions on inhaled virus load

Our study examined various postures and positions that people may stand while in an elevator, including two postures and three different source locations. The results and analysis of cases 2 to 5 are presented in this section.

Fig. 10(a) illustrates the number of virus copies inhaled by each person in Case 2, where only the standing postures of D and E were altered. The other boundary conditions were identical to those in Case 1. Unlike Case 1, the particles initially reached the breathing zone of person C before person D, due to the significant impact of the changes in the standing postures of D and E on the airflow within the elevator. Before the time of 50 s, person C had the highest accumulated dose due to their proximity to the infected person. However, over the 2-min duration of the ride, person D inhaled the most virus copies with a total of 587, as many particles initially traveled upward before descending to the breathing zone of that person.

Fig. 10(b) displays the amount of virus copies inhaled by each person in both Case 3 and Case 4, where person C was designated as the infected person. The solid and dashed lines represent the results for standing postures I and II, respectively. Compared to Case 1, the number of virus copies inhaled by person E greatly increased in Case 3. This was because when the infected person stands in position C, the particles generated by coughing travel upward due to the thermal plume before descending with the airflow. When comparing Cases 3 and 4, it is shown that the number of inhaled particles in standing posture I was greater than that of standing posture II. This was because the downward airflow created by the inlet suppressed the upward dispersion of the particles. The highest number of inhaled virus copies for Cases 3 and 4 were 567 and 237, respectively. According to Fig. 10(b), although persons D and E are positioned similarly relative to person C, they did not inhale the same virus. This is because the breathing curves for them are not exactly the same, as shown in Fig. 2(b). In addition, the turbulent dispersion of particles was modeled using the discrete random walk method, which may introduce inaccuracies due to the random fluctuations of computed concentrations [59].

Fig. 10(c) illustrates the amount of virus copies inhaled by each person in Case 5. When the standing postures of person D and person E

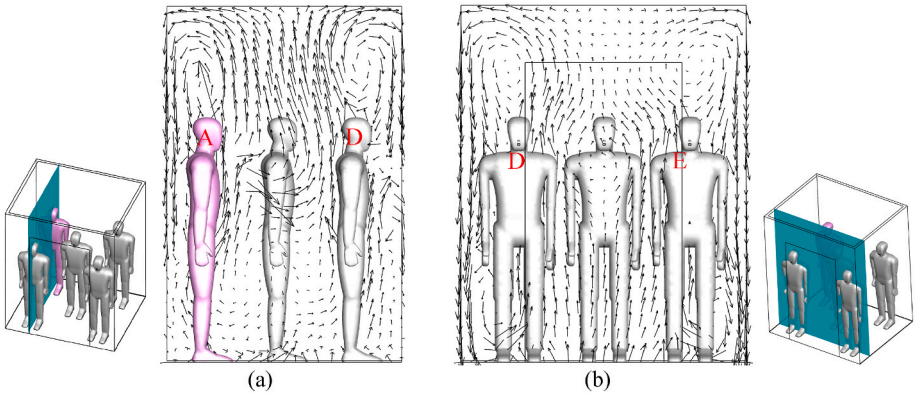

Fig. 8. Velocity distributions in the elevator of Case 1 at t = 120 s: (a) airflow in the surface across infected person A and person D, (b) airflow in the surface across persons D and E.

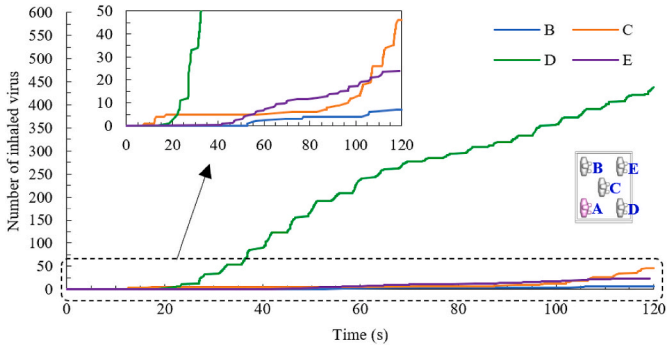

Fig. 9. Accumulated dose for each person in Case 1.

were altered, the downward airflow from the inlet on top of person D and E inclined towards person C because there was less resistance between person D and E compared to standing posture I. As a result, particles were more likely to spread into the breathing zone of person C. Person C inhaled the largest amount of virus copies with a total of 1186.

Fig. 11 compares the air velocity distributions of different cases with 3 ACH. Fig. 11(a) depicts the velocity distributions in the elevator of Case 2. It demonstrates that the airflow distributions were almost symmetrical due to the geometry symmetry. Two vortexes were formed on the upper part of the person. However, the airflow distributions on the lower part of the elevator were significantly affected by persons D and E. Their shoulders blocked the downward airflow and caused the flow direction to change, forming two vortexes on the lower part of the elevator. Fig. 11(b) depicts the velocity distributions in the elevator of Case 3. Here, the thermal plume generated from the persons and the downward airflow from the inlets caused two vortexes on the upper part of the elevator. The airflow distributions were similar to those of Case 1 with the same standing postures. This is because the difference in particle information and cough-generated airflow boundary conditions at the noses of different persons would not essentially change the airflow pattern due to the short coughing time. Fig. 11(c) and (d) demonstrate the velocity distributions in the elevator of Case 4 and Case 5, which were similar to those of Case 2.

3.4. Impact of ventilation rates on inhaled virus load

The amount of air that was ventilated into an elevator could vary depending on the type of ventilation system. The baseline case in this study used a ventilation rate of 0.007 m^3/s (3 ACH). This investigation also compared another flow rate of 0.069 m^3/s (30 ACH), which was equivalent to mechanical ventilation. Table 4 summarizes the amount of inhaled virus copies for each person in various cases. Generally, as the

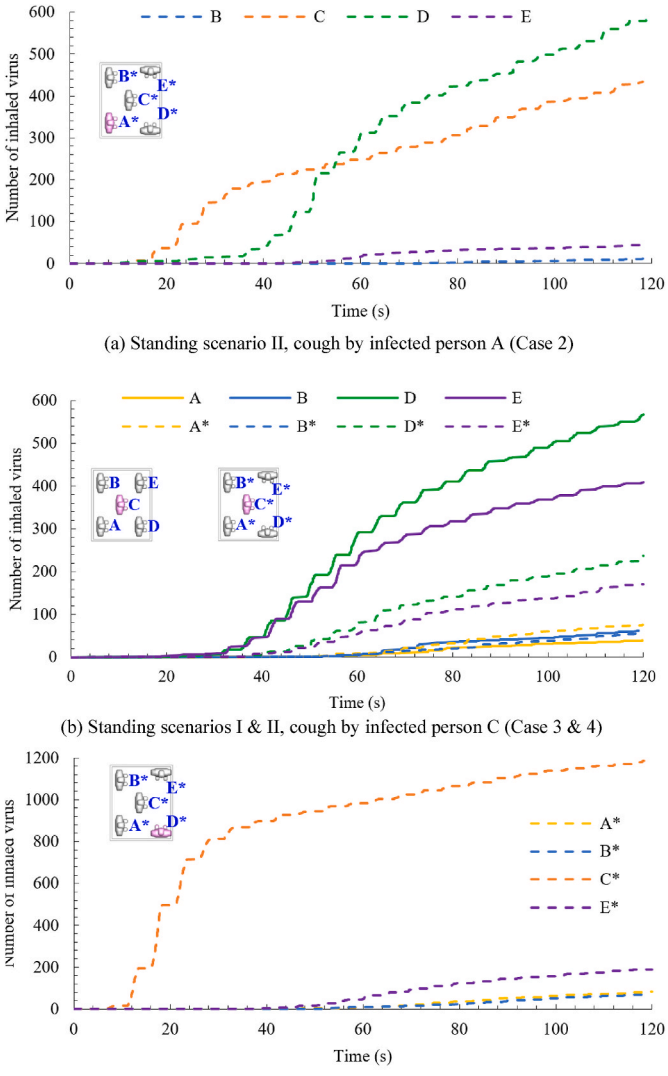

Fig. 10. Comparison of the accumulated inhaled virus in different cases for 3 ACH.

ventilation rate increased, the average inhaled virus copies for other persons decreased, as Case 7–10 showed. However, in Case 6 when the infected person stood in position A with standing posture I, the inhaled virus copies for persons in the 30 ACH scenario were higher than that of

the 3 ACH scenario. This was because the larger momentum of air from the inlet causes particles to travel more quickly to the breathing zones of other persons. As shown in Fig. 12(a), some particles have reached the floor in front of person D at t = 20s, while in Case 1, particles only reached the head region of person D at the same time, as shown in Fig. 7.

Additionally, the supply air went down to the floor first and then went upward in front of person A for Case 6, as shown in Fig. 13(a). The high air velocity blew particles away, resulting in an increase in inhaled virus copies for the susceptible persons of Case 6 compared to Case 1. The highest inhaled virus copies for Case 6 were 509.

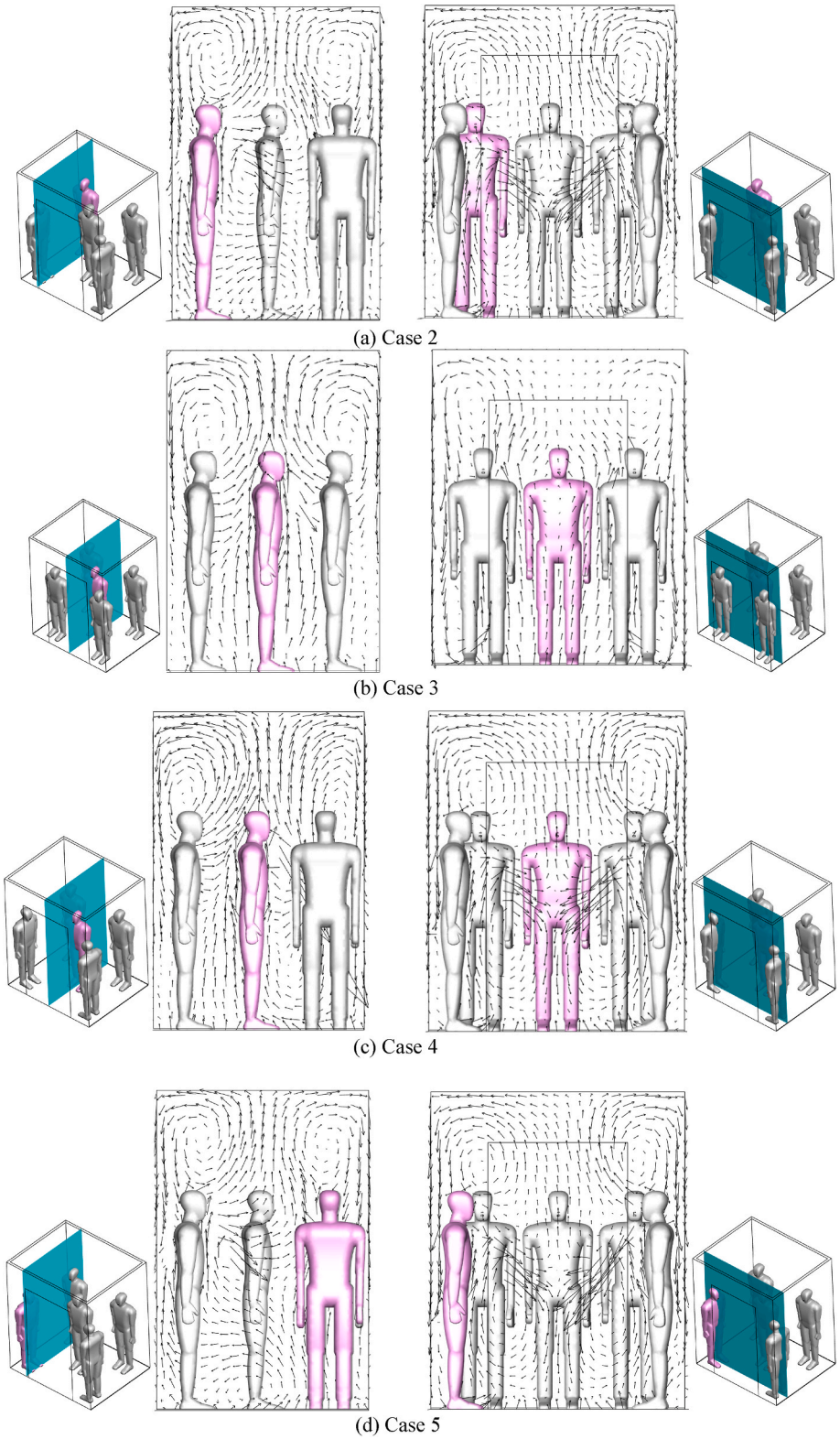

Fig. 11. Velocity distributions in the elevator of different cases for 3 ACH at t = 120 s: Case 2 to Case 5. (The green surfaces show the positions of the vectors.). (For interpretation of the references to color in this figure legend, the reader is referred to the Web version of this article.)

In Case 7, the inhaled virus copies of person C decreased significantly compared to Case 2. This was because the air velocity around person C was smaller, causing particles to more easily concentrate in the breathing zone in Case 2. As shown in Fig. 12(b), at t = 20s and t = 40s, there were fewer particles in the breathing zone of person C compared to Case 2. The inhaled virus copies for other persons also decreased due to the increased ventilation rate.

In Case 8 and Case 9, the increased airflow rate caused a decrease in the number of inhaled virus copies for persons D and E. However, for other persons standing behind the infected person, the number of inhaled virus copies may increase. This was because the higher air velocity in the elevator, as shown in Fig. 12(c) and (d), with the 30 ACH scenario, caused the particles to spread farther compared to the smaller airflow rate of 3 ACH.

Fig. 12(e) shows the particle distribution in the elevator for Case 10. Similarly, the particles were dispersed over a larger area in Case 10 compared to Case 5. A higher ventilation rate could reduce the concentration of particles more quickly, but it also caused the particles to spread further. Thus, it may lead to an increase in the number of inhaled virus copies for other persons.

Table 4 summarizes the inhaled virus copies for each person in different cases. In general, using mechanical ventilation with a flow rate of 30 ACH reduced the risk of infection of COVID-19 in an elevator. The highest number of inhaled virus copies for 3 ACH scenarios was between 237 and 1186, while for 30 ACH scenarios, the highest number was between 153 and 509. More detailed information on inhaled virus copies over time for each person in Cases 6 to 10 can be found in the Appendix.

Fig. 13 compares the air velocity distributions of different cases with 30 ACH. Fig. 13(a) depicts the velocity distributions in the elevator of Case 6. The air velocity in the elevator was higher than that of Case 1, as shown in Fig. 8. The downward airflow from the inlets reaches the floor without forming any vortexes on the upper part of the elevator due to the large air momentum. Fig. 13(b) shows the velocity distributions in the elevator of Case 7. The airflow distribution was similar to that of Case 2 but with larger air velocities. Moreover, Case 8 was almost the same as Case 3; and Cases 9 and 10 were nearly the same as Cases 4 and 5, respectively. The major difference was that the air velocity for 30 ACH was larger than that of 3 ACH. The air velocity in the breathing zone for 3 and 30 ACH was around 0.08 m/s and 0.15 m/s, respectively. With 30 ACH, the downward airflow from the inlets could reach the floor. Some of the air was exhausted from the outlets while some others bounced upward to the breathing zone. This resulted in a significant decrease in air velocity due to the hitting effect.

3.5. Impact of wearing masks on inhaled virus load

We also investigated the impact of wearing masks on inhaled virus load, as people may wear masks in the elevator. The results of cases 11 to 13 showed that wearing masks can effectively reduce the infection risk of COVID-19 in the elevator. Fig. 14 shows the accumulated number of virus copies inhaled by each person in the cases of coughing while wearing a mask, which exhibited the same trend as the cases without masks in Fig. 10. However, thanks to the filtering of large particles and the suppressed coughing velocities, the number of inhaled virus copies for susceptible persons was much lower than the no mask cases. Table 5 summarizes the inhaled virus copies for each person of cases with and without wearing masks, showing that the highest number of inhaled copies can be effectively reduced from 237 to 1186 to 74 to 155 when wearing surgical masks. Our investigation found that wearing masks properly by the infected person can reduce the inhaled virus copies by 70%–90%, which is consistent with the previous investigation [26]. One can use the reduction efficiency scaling to estimate the number of inhaled viruses for other scenarios.

Table 4
Summary of the inhaled virus copies for each person in different cases. (Ave. Means the average value of four susceptible persons.)

Case	ACH	Infected person	A	B	C	D	E	Ave.
1	3	A	0	7	46	438	24	129
2	3	A	0	11	433	587	44	269
3	3	C	39	61	0	567	408	269
4	3	C	76	56	0	237	170	135
5	3	D	84	72	1186	0	190	383
6	30	A	0	11	111	509	38	167
7	30	A	0	11	79	438	21	137
8	30	C	63	57	0	381	362	216
9	30	C	142	84	0	153	106	121
10	30	D	170	50	476	0	87	196

3.6. Impact of different riding time on inhaled virus load

This study simulated a 120-s elevator ride. In reality, people may stay in the elevators for varying durations. Therefore, we further calculated the inhaled virus copies for each person with shorter rides of 30 s and 60 s, as shown in Table 6. We found that only person C in Case 5 may be at risk of infection if the riding time was less than 60 s. Note that according to [60], different virus variants such as Alpha, Delta, and Omicron may shed more viral RNA copies into exhaled aerosols than other variants, making the number of virus copies required for infection dependent on the virus subtype. Additionally, this investigation assumed the infected person coughed once. Whereas in reality, the infected person may cough several times. The simulated results can be overlaid multiple times to estimate the inhaled virus copies for multiple coughing [61].

4. Discussions

This study used a uniform manikin model for all the persons to estimate the risk of COVID-19 infection. Future studies should take into account the diversity of persons in terms of gender, age, height, and weight. Additionally, this study only considered two standing postures and three different source locations due to limitations in computing resources. Additional scenarios should be explored in future studies, such as the impact of different social distancing measures and the facing positions of people with varying loading capacities. Moreover, the standing positions may be random rather than symmetrical in the cab. Previous investigations [62,63] have found that the asymmetric geometry may lead to asymmetric airflow and the cross-transport of pollutants. Therefore, future investigations should examine the influence of different random standing postures on airflow and particle transmission. This study assumed that only the infected person was wearing a surgical mask in the elevator, and the infection risk could be significantly reduced. When all persons wore surgical masks, the inhaled dose could be further reduced [45]. Previous research [29,64] has also shown that wearing masks could effectively reduce the risk of infection. Therefore, it is recommended to wear a mask in elevators for protection against COVID-19.

This investigation assumed that the elevator cab was clean when the simulation started. However, in reality, particles can settle on various surfaces in the elevator, including the person in front of the infected person, the floor, the elevator buttons and the walls, as Fig. 15 depicts. Additionally, some particles may remain suspended in the air in the elevator. Since elevators are frequently used in buildings, it is possible that the cab may contain the COVID-19 virus for long time. Further research is needed to answer the questions: if elevator cabs should be sanitized before each ride, and if air purification systems should be installed. Additionally, more research should be done to understand the risk of infection through contact with surfaces [65].

This investigation utilized a mixing ventilation system that bring in air from the ceiling perimeter of the elevator which affected the spread of COVID-19. The results in Section 3.4 showed that increasing the ventilation rate did not always decrease the risk of infection proportionally, and in some cases, it even increased the risk due to uneven

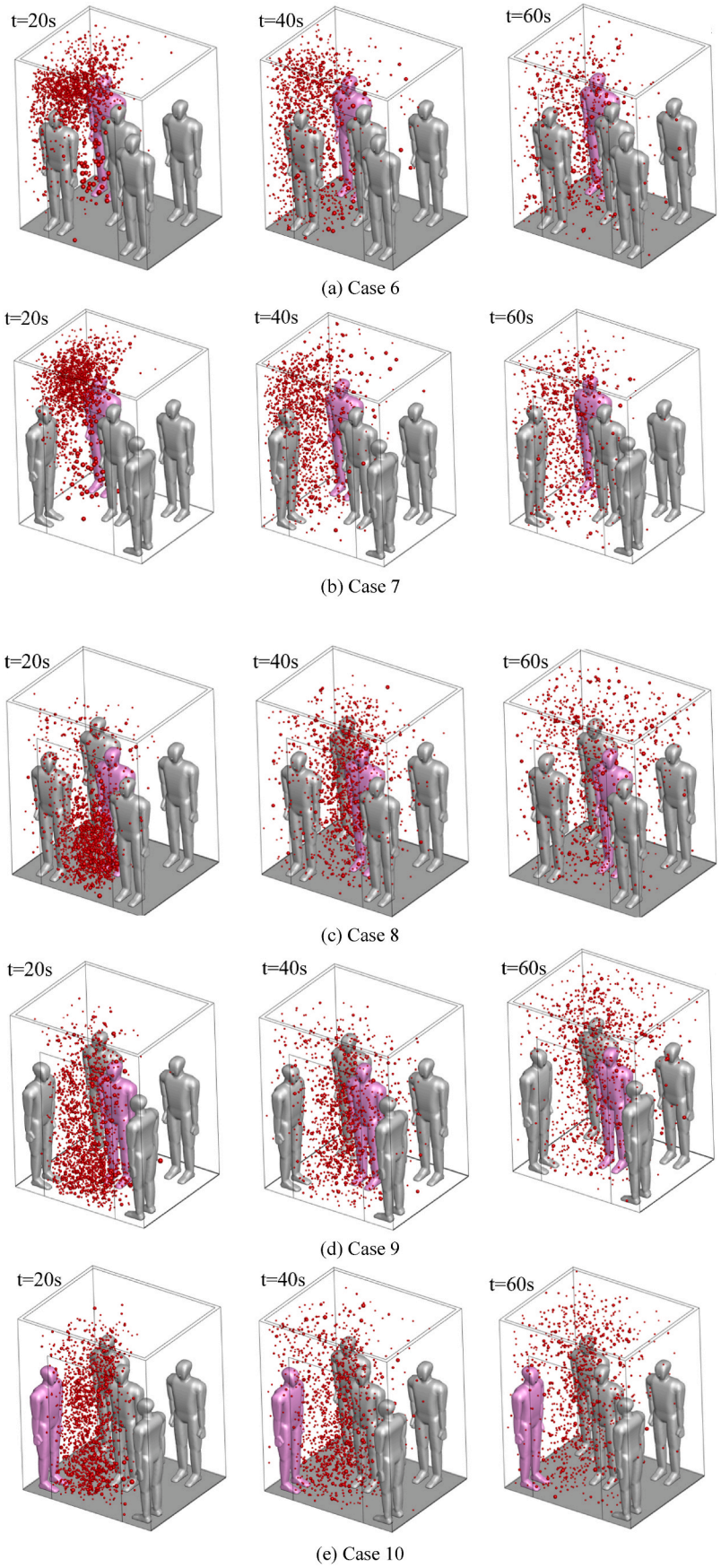

Fig. 12. Distributions of droplet nuclei and air velocity in different cases: Case 6 to Case 10.

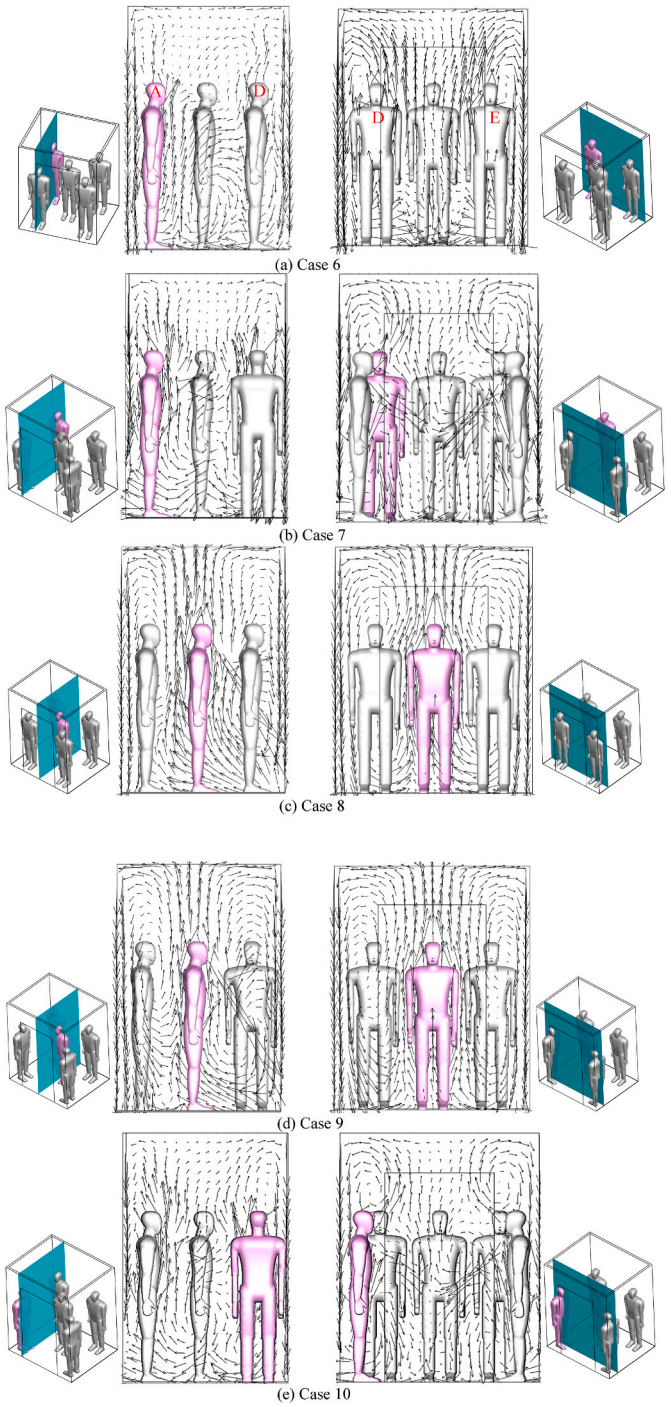

Fig. 13. Velocity distributions in the elevator of different cases for 30 ACH at t = 120 s: Case 6 to Case 10.

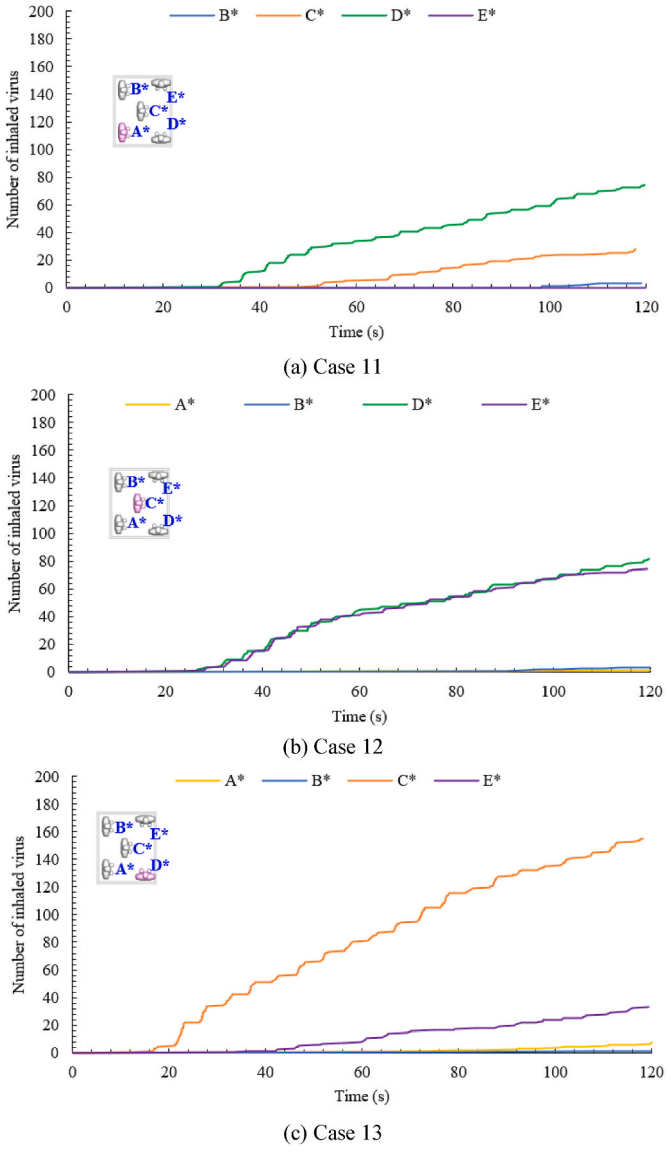

Fig. 14. Comparison of the accumulated inhaled virus in the mask covered coughing case: Case 11 to Case 13.

Table 5
Summary of the inhaled virus copies for each person in cases with and without masks. (Ave. Means the average value of four susceptible persons.)

Mask	Case	ACH	A	B	C	D	E	Ave.
None	2	3	0	11	433	587	44	269
	4	3	76	56	0	237	170	135
	5	3	84	72	1186	0	190	383
Surgical mask	11	3	0	0	28	74	0	26
	12	3	0	3	0	82	75	40
	13	3	8	1	155	0	33	39

particle distribution. The mixing ventilation system is not suitable for elevators unless higher ventilation rates were implemented. This study only compared two different ventilation rates. It may be possible to test cases with much higher ventilation rates in the future. Previous research has shown that the direction of air supply can impact particle transmission in an elevator cab [24,25]. We suggest that more research is needed to determine the best ventilation system design to decrease the risk of infection [66], as well as to consider factors such as the direction of air supply and when the infected person coughs during the ride.

This investigation used the particular spectrum as the source information to conduct the CFD simulation. There are several investigations [67,68] that provide information on particle size and number in cough. Using different particular spectrum may result in different simulated outcomes, which should be further investigated. In addition, this study calculated the number of virus copies that each person in the elevator would inhale under different scenarios. We used a model that took into account the number of particles inhaled and the virus load on those particles. However, it should be noted that this model assumed that all inhaled particles were biologically active and able to transmit the virus, which may not be entirely accurate. This simplification is commonly

Table 6
Summary of the inhaled virus copies by each person in different cases for different riding times.

Riding time	Case	ACH	Infected person	A	B	C	D	E
30s	1	3	A	0	0	5	34	0
	2	3	A	0	0	146	14	0
	3	3	C	0	0	0	1	1
	4	3	C	0	0	0	1	1
	5	3	D	0	0	812	0	1
	6	30	A	0	0	0	126	0
	7	30	A	0	0	5	17	0
	8	30	C	0	0	0	131	111
	9	30	C	0	0	0	16	5
	10	30	D	0	0	66	0	3
	11	3	A	0	0	0	0	0
	12	3	C	0	0	0	4	4
	13	3	D	0	0	34	0	0
60s	1	3	A	0	3	6	240	7
	2	3	A	0	0	247	312	20
	3	3	C	9	7	0	82	57
	4	3	C	10	6	0	81	55
	5	3	D	9	9	985	0	144
	6	30	A	0	0	17	370	12
	7	30	A	0	0	13	266	6
	8	30	C	23	9	0	239	225
	9	30	C	63	34	0	60	35
	10	30	D	68	8	275	0	21
	11	3	A	0	0	6	35	0
	12	3	C	0	0	0	45	41
	13	3	D	1	0	81	0	8

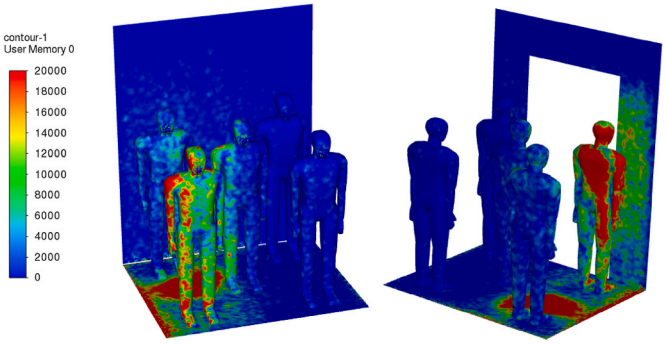

Fig. 15. Particle number deposition on different surfaces in the elevator (Left: front view; Right: back view. Person A is the infected person).

used because modeling and predicting the biology of transmission is challenging. More research is needed to better understand the role of particle biology and environmental factors in the transmission and infection risk of COVID-19 [69].

5. Conclusions

In this study, the validated CFD model was employed to investigate the potential transmission of COVID-19 through coughing in an elevator. We computed the number of virus particles inhaled by susceptible persons during a 2-min ride in the elevator. The study led to the following conclusions.

- For the baseline base, the virus particles reached the breathing zone of person D at 20 s. This person inhaled 438 virus copies during a 2-min elevator ride, which could result in infection. On the other hand, the number of virus copies inhaled by the remaining three persons was less than 50, which may not lead to infection.
- The results revealed that the position of the source and the standing posture significantly impacted the spread of particles in the elevator. In both standing postures, the person standing in front of or beside the infected person was found to inhale the highest number of virus copies, which could reach 1186 during a 2-min elevator ride.
- The study evaluated the effect of various ventilation rates on the risk of infection. The results showed that using a mechanical ventilation system with a flow rate of 30 air ACH reduced the COVID-19 transmission in the elevator. In 3 ACH scenarios, the highest number of inhaled virus copies ranged from 237 to 1186, while in the 30 ACH scenarios, the highest number was reduced to 153 to 509.
- The study investigated the impact of wearing surgical masks on the risk of infection. In 3 ACH scenarios with standing posture II, wearing surgical masks was found to reduce the highest number of inhaled virus copies to 74 to 155.

CRediT authorship contribution statement

Sumei Liu: Writing – review & editing, Writing – original draft, Software, Project administration, Methodology, Investigation, Funding acquisition, Conceptualization. **Zhipeng Deng:** Writing – review & editing, Writing – original draft, Methodology.

Declaration of competing interest

The authors declare that they have no known competing financial interests or personal relationships that could have appeared to influence the work reported in this paper.

Data availability

Data will be made available on request.

Acknowledgment

The authors would like to acknowledge the support from the National Key R&D Program from the Ministry of Science and Technology, China, on “Comprehensive control of air, soil and groundwater pollution” through Grant No. 2022YFC3702803 and by the National Natural Science Foundation of China (NSFC) through grant No. 52108084.

Appendix A. Supplementary data

Supplementary data to this article can be found online at https://doi.org/10.1016/j.buildenv.2023.110343.

Appendix I. The airflow distributions in the elevator of Case 1 over time

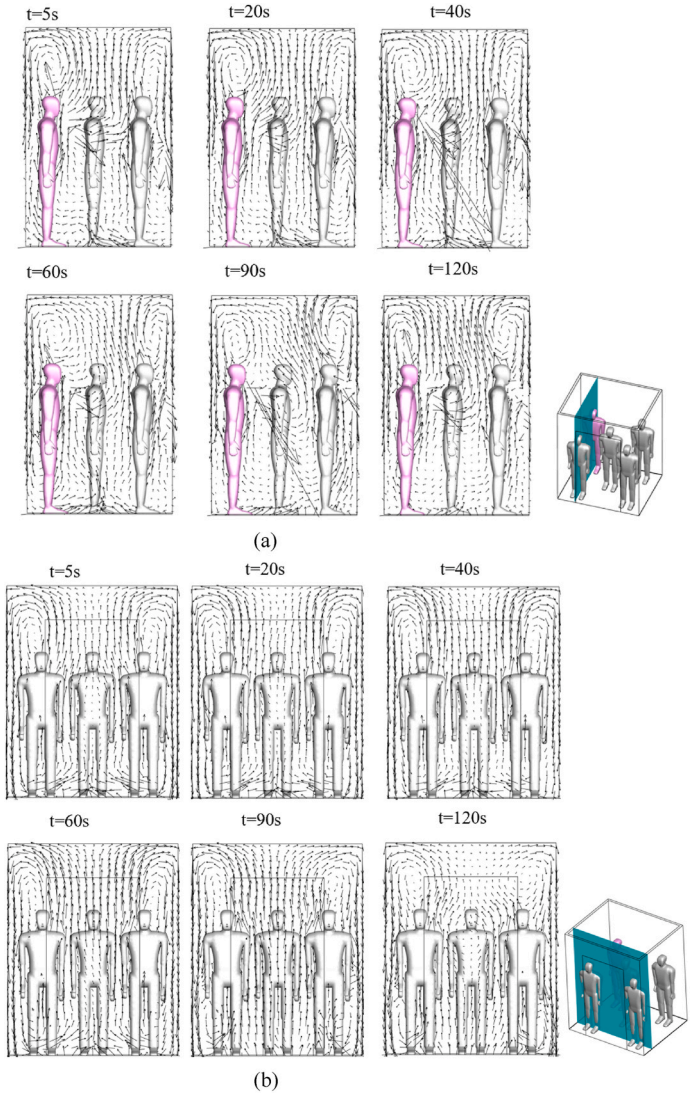

Fig. A1. The airflow distributions in the elevator of Case 1 over time: (a) airflow in the surface across infected person A and person D, (b) airflow in the surface across persons D and E.

Appendix II. The accumulated inhaled virus for each person of Case 6 to Case 10

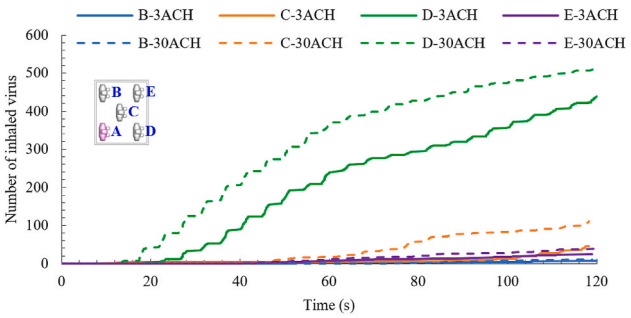

Fig. A2. Number of virus copies inhaled by each person in different cases with different ventilation rates.

References

[1] G. La Rosa, M. Fratini, S.D. Libera, M. Iaconelli, M. Muscillo, Viral infections acquired indoors through airborne, droplet or contact transmission, Annali dell'Istituto superiore di sanita 49 (2013) 124–132.

[2] S. Tang, Y. Mao, R.M. Jones, Q. Tan, J.S. Ji, N. Li, J. Shen, Y. Lv, L. Pan, P. Ding, X. Wang, Y. Wang, R. Maclntyre, X. Shi, Aerosol transmission of SARS-CoV-2? Evidence, prevention and control, Environ. Int. 144 (2020), 106039.

[3] Y. Li, H. Qian, J. Hang, X. Chen, P. Cheng, H. Ling, S. Wang, P. Liang, J. Li, S. Xiao, J. Wei, L. Liu, B.J. Cowling, M. Kang, Probable airborne transmission of SARS-CoV-2 in a poorly ventilated restaurant, Build. Environ. 196 (2021), 107788.

[4] X. Zhao, S. Liu, Y. Yin, T. Zhang, Q. Chen, Airborne transmission of COVID-19 virus in enclosed spaces: an overview of research methods, Indoor Air 32 (6) (2022), e13056.

[5] J. Chen, H. He, W. Cheng, Y. Liu, Z. Sun, C. Chai, Q. Kong, W. Sun, J. Zhai, S. Guo, X. Shi, J. Wang, E. Chen, Z. Chen, Potential transmission of SARS-CoV-2 on a flight from Singapore to Hangzhou, China: an epidemiological investigation, Trav. Med. Infect. Dis. 36 (2020), 101816.

[6] C. Xie, H. Zhao, K. Li, Z. Zhang, X. Lu, H. Peng, D. Wang, J. Chen, X. Zhang, D. Wu, Y. Gu, J. Yuan, L. Zhang, J. Lu, The evidence of indirect transmission of SARS-CoV-2 reported in Guangzhou, China, BMC Publ. Health 20 (1) (2020) 1–9.

[7] J. Yan, M. Grantham, J. Pantelic, P.J. Bueno de Mesquita, B. Albert, F. Liu, S. Ehrman, D.K. Milton, Emit Consortium, Infectious virus in exhaled breath of symptomatic seasonal influenza cases from a college community, Proc. Natl. Acad. Sci. USA 115 (5) (2018) 1081–1086.

[8] X. Xie, Y. Li, H. Sun, L. Liu, Exhaled droplets due to talking and coughing, J. R. Soc. Interface 6 (suppl_6) (2009) S703–S714.

[9] S. Park, Y. Choi, D. Song, E.K. Kim, Natural ventilation strategy and related issues to prevent coronavirus disease 2019 (COVID-19) airborne transmission in a school building, Sci. Total Environ. 789 (2021), 147764.

[10] T. Dbouk, D. Drikakis, On coughing and airborne droplet transmission to humans, Phys. Fluids 32 (5) (2020), 053310.

[11] R.K. Bhagat, M.S.D. Wykes, S.B. Dalziel, P.F. Linden, Effects of ventilation on the indoor spread of COVID-19, J. Fluid Mech. (2020) 903.

[12] S. Liu, M. Koupriyanov, D. Paskaruk, G. Fediuk, Q. Chen, Investigation of airborne particle exposure in an office with mixing and displacement ventilation, Sustain. Cities Soc. 79 (2022), 103718.

[13] International Standards Organization, ISO 8100-1 Lifts for the Transport of Persons and Goods — Part 1: Passenger and Goods Passenger Lifts, 2019.

[14] European Committee for Standardization (EN 81) Safety Rules for the Construction and Installation of Lifts - Lifts for the Transport of Persons and Goods - Part 20: Passenger and Goods Passenger Lifts.

[15] The American Society of Mechanical Engineers. ASME A17.1/CSA B44-16. Safety Code for Elevators and Escalators.

[16] T. Zhang, M. Fan, S. Liu, Impact of seat inclination and misalignment on airborne pollutant transport in a single-aisle aircraft cabin, Appl. Sci. 12 (9) (2022) 4538.

[17] H. Qian, Y. Li, P.V. Nielsen, C.E. Hyldgaard, Dispersion of exhalation pollutants in a two-bed hospital ward with a downward ventilation system, Build. Environ. 43 (3) (2008) 344–354.

[18] S. Mazumdar, Y. Yin, A. Guity, P. Marmion, B. Gulick, Q. Chen, Impact of moving objects on contaminant concentration distributions in an inpatient ward with displacement ventilation, HVAC R Res. 16 (5) (2010) 545–563.

[19] Y. Wang, Z. Deng, D. Shi, How effective is a mask in preventing COVID-19 infection? Med. Dev. Sensor 4 (1) (2021), e10163.

[20] T. Li, Y. Liu, M. Li, et al., Mask or no mask for COVID-19: a public health and market study, PLoS One 15 (8) (2020), e0237691.

[21] S. Shao, D. Zhou, R. He, J. Li, S. Zou, K. Mallery, S. Kumar, S. Yang, J. Hong, Risk assessment of airborne transmission of COVID-19 by asymptomatic individuals under different practical settings, J. Aerosol Sci. 151 (2021), 105661.

[22] T. Dbouk, D. Drikakis, On airborne virus transmission in elevators and confined spaces, Phys. Fluids 33 (1) (2021), 011905.

[23] R. Biswas, A. Pal, R. Pal, S. Sarkar, A. Mukhopadhyay, Risk assessment of COVID infection by respiratory droplets from cough for various ventilation scenarios inside an elevator: an OpenFOAM-based computational fluid dynamics analysis, Phys. Fluids 34 (1) (2022), 013318.

[24] N. Sen, Transmission and evaporation of cough droplets in an elevator: numerical simulations of some possible scenarios, Phys. Fluids 33 (3) (2021), 033311.

[25] S. Liu, X. Zhao, S.R. Nichols, M.W. Bonilha, T. Derwinski, J.T. Auxier, Q. Chen, Evaluation of airborne particle exposure for riding elevators, Build. Environ. 207 (2022), 108543.

[26] C. Du, Q. Chen, Virus transport and infection evaluation in a passenger elevator with a COVID-19 patient, Indoor Air 32 (10) (2022), e13125.

[27] N. Zeng, Z. Li, S. Ng, et al., Epidemiology reveals mask wearing by the public is crucial for COVID-19 control, Med. Microecol. 4 (2020), 100015.

[28] O. Falodun, N. Medugu, L. Sabir, et al., An epidemiological study on face masks and acne in a Nigerian population, PLoS One 17 (5) (2022), e0268224.

[29] Z. Deng, Q. Chen, What is suitable social distancing for people wearing face masks during the COVID-19 pandemic? Indoor Air 32 (1) (2022), e12935.

[30] Standard 62.1-2007 User's Manual, American Society of Heating, Refrigerating and Air-Conditioning Engineers, Inc., Atlanta, GA, 2007.

[31] C.Y.H. Chao, M.P. Wan, L. Morawska, B.R. Johnson, M. Hargreaves, K. Mengersen, S. Corbett, X. Xie, D. Katoshevski, Characterization of expiration air jets and particle size distributions immediately at the mouth opening, J. Aerosol Sci. 40 (2) (2009) 122–133.

[32] S. Yang, G.W.M. Lee, C.M. Chen, C.C. Wu, K.P. Yu, The size and concentration of droplets generated by coughing in human subjects, J. Aerosol Med. 20 (4) (2007) 484–494.

[33] J. Redrow, S. Mao, I. Celik, et al., Modeling the evaporation and dispersion of airborne sputum droplets expelled from a human cough, Build. Environ. 46 (10) (2011) 2042–2051.

[34] X. Li, Y. Shang, Y. Yan, et al., Modelling of evaporation of cough droplets in inhomogeneous humidity fields using the multi-component Eulerian-Lagrangian approach, Build. Environ. 128 (2018) 68–76.

[35] J.K. Gupta, C.H. Lin, Q. Chen, Transport of expiratory droplets in an aircraft cabin, Indoor Air 21 (1) (2011) 3–11.

[36] M. Nicas, W.W. Nazaroff, A. Hubbard, Toward understanding the risk of secondary airborne infection: emission of respirable pathogens, J. Occup. Environ. Hyg. 2 (3) (2005) 143–154.

[37] G.R. Johnson, L. Morawska, Z.D. Ristovski, M. Hargreaves, K. Mengersen, C.Y. H. Chao, M.P. Wan, Y. Li, X. Xie, D. Katoshevski, S. Corbett, Modality of human expired aerosol size distributions, J. Aerosol Sci. 42 (12) (2011) 839–851.

[38] Y. Pan, D. Zhang, P. Yang, L.L. Poon, Q. Wang, Viral load of SARS-CoV-2 in clinical samples, Lancet Infect. Dis. 20 (4) (2020) 411–412.

[39] K.K.W. To, O.T.Y. Tsang, C.C.Y. Yip, K.K. Chan, T.C. Wu, J.M.C. Chan, W.S. Leung, T.S.H. Chik, C.Y.C. Choi, D.H. Kandamby, D.C. Lung, A.R. Tam, R.W.S. Poon, A.Y. F. Fung, I.F.N. Huang, V.C.C. Cheng, J.F.W. Chan, K.Y. Yuen, Consistent detection of 2019 novel coronavirus in saliva, Clin. Infect. Dis. 71 (15) (2020) 841–843.

[40] W.G. Lindsley, F.M. Blachere, R.E. Thewlis, A. Vishnu, K.A. Davis, G. Cao, J. E. Palmer, K.E. Clark, M.A. Fisher, R. Khakoo, D.H. Beezhold, Measurements of airborne influenza virus in aerosol particles from human coughs, PLoS One 5 (11) (2010), e15100.

[41] W. Wang, F. Wang, D. Lai, Q. Chen, Evaluation of SARS-COV-2 transmission and infection in airliner cabins, Indoor Air 32 (1) (2022), e12979.

[42] J.K. Gupta, C.H. Lin, Q. Chen, Characterizing exhaled airflow from breathing and talking, Indoor Air 20 (1) (2010) 31–39.

[43] J.K. Gupta, C.H. Lin, Q. Chen, Flow dynamics and characterization of a cough, Indoor Air 19 (6) (2009) 517–525.

[44] C. Chen, C.H. Lin, Z. Jiang, et al., Simplified models for exhaled airflow from a cough with the mouth covered, Indoor Air 24 (6) (2014) 580–591.

[45] J. Pan, C. Harb, W. Leng, et al., Inward and outward effectiveness of cloth masks, a surgical mask, and a face shield, Aerosol. Sci. Technol. 55 (6) (2021) 718–733.

[46] S. Liu, L. Xu, J. Chao, C. Shen, J. Liu, H. Sun, X. Xiao, G. Nan, Thermal environment around passengers in an aircraft cabin, HVAC R Res. 19 (5) (2013) 627–634.

[47] J.H. Klote, G. Tamura, Elevator piston effect and the smoke problem, Fire Saf. J. 11 (3) (1986) 227–233.

[48] M. Prentiss, A. Chu, K.K. Berggren, Superspreading events without superspreaders: using high attack rate events to estimate Nº for airborne transmission of COVID-19, medRxiv (2020).

[49] M. Riediker, L. Briceno-Ayala, G. Ichihara, et al., Higher viral load and infectivity increase risk of aerosol transmission for Delta and Omicron variants of SARS-CoV-2, Swiss Med. Wkly. 152 (102) (2022) w30133-w30133.

[50] T.H. Shih, W.W. Liou, A. Shabbir, Z. Yang, J. Zhu, A new k-ε eddy viscosity model for high Reynolds number turbulent flows, Comput. Fluids 24 (3) (1995) 227–238.

[51] Z. Zhang, W. Zhang, Z.J. Zhai, Q. Chen, Evaluation of various turbulence models in predicting airflow and turbulence in enclosed environments by CFD: Part 2 - comparison with experimental data from literature, HVAC R Res. 13 (6) (2007) 871–886.

[52] S.B. Pope, Turbulent Flows, Cambridge University Press, Cambridge, UK, 2000, p. 771. Combustion and Flame, 2001, 4(125): 1361-1362.

[53] V. Yakhot, S.A. Orszag, Renormalization group analysis of turbulence. I. Basic theory, J. Sci. Comput. 1 (1) (1986) 3–51.

[54] M.D. Allen, O.G. Raabe, Slip correction measurements of spherical solid aerosol particles in an improved Millikan apparatus, Aerosol. Sci. Technol. 4 (3) (1985) 269–286.

[55] S.A.J. Morsi, A.J. Alexander, An investigation of particle trajectories in two-phase flow systems, J. Fluid Mech. 55 (2) (1972) 193–208.

[56] ANSYS Fluent Theory Guide 21 R1, ANSYS, Inc., Canonsburg, Pennsylvania, USA, 2021.

[57] Z. Zhang, Q. Chen, Experimental measurements and numerical simulations of particle transport and distribution in ventilated rooms, Atmos. Environ. 40 (18) (2006) 3396–3408.

[58] S. Liu, M. Koupriyanov, D. Paskaruk, et al., Investigation of airborne particle exposure in an office with mixing and displacement ventilation, Sustain. Cities Soc. 79 (2022), 103718.

[59] P. Salamon, D. Fernàndez-Garcia, J.J. Gómez-Hernández, A review and numerical assessment of the random walk particle tracking method, J. Contam. Hydrol. 87 (3–4) (2006) 277–305.

[60] J. Lai, K.K. Coleman, S.H.S. Tai, et al., Exhaled Breath Aerosol Shedding of Highly Transmissible versus Prior Severe Acute Respiratory Syndrome Coronavirus 2 Variants, Clinical Infectious Diseases, 2022, ciac846.

[61] J.K. Gupta, Respiratory Exhalation/inhalation Models and Prediction of Airborne Infection Risk in an Aircraft Cabin, Purdue University, 2010.
[62] Z. Zhang, X. Chen, S. Mazumdar, et al., Experimental and numerical investigation of airflow and contaminant transport in an airliner cabin mockup, Build. Environ. 44 (1) (2009) 85–94.
[63] S. Mazumdar, Q. Chen, Influence of cabin conditions on placement and response of contaminant detection sensors in a commercial aircraft, J. Environ. Monit. 10 (1) (2008) 71–81.
[64] J. Howard, A. Huang, Z. Li, Z. Tufekci, V. Zdimal, H.M. van der Westhuizen, A. von Delft, A. Price, L. Fridman, L.H. Tang, V. Tang, G.L. Watson, C.E. Bax, R. Shaikh, F. Questier, D. Hernandez, L.F. Chu, C. Ramirez, A.W. Rimoin, An evidence review of face masks against COVID-19, Proc. Natl. Acad. Sci. USA 118 (4) (2021), e2014564118.
[65] J. Ren, M. Tang, A. Novoselac, Experimental study to quantify airborne particle deposition onto and resuspension from clothing using a fluorescent-tracking method, Build. Environ. 209 (2022), 108580.
[66] X. Dai, S. Cheng, A. Chong, Deciphering optimal mixed-mode ventilation in the tropics using reinforcement learning with explainable artificial intelligence, Energy Build. 278 (2023), 112629.
[67] X. Xie, Y. Li, H. Sun, et al., Exhaled droplets due to talking and coughing, J. R. Soc. Interface 6 (suppl_6) (2009) S703–S714.
[68] S. Yang, G.W.M. Lee, C.M. Chen, et al., The size and concentration of droplets generated by coughing in human subjects, J. Aerosol Med. 20 (4) (2007) 484–494.
[69] C. Duchaine, C.J. Roy, Bioaerosols and airborne transmission: integrating biological complexity into our perspective, Sci. Total Environ. 825 (2022), 154117.